Amplification of Chirality: The "Sergeants and Soldiers" Principle Applied to Dynamic Hydrogen-Bonded Assemblies†

Leonard J. Prins, Peter Timmerman,* and David N. Reinhoudt*

Contribution from the Laboratory of Supramolecular Chemistry and Technology, MESA+ Research Institute, University of Twente, P.O. Box 217, 7500 AE, Enschede, The Netherlands

Received March 6, 2001

Abstract: The amplification of supramolecular chirality has been studied in dynamic chiral hydrogen-bonded assemblies $\mathbf{1}_3\cdot(CA)_6$ using "Sergeants and Soldiers" experiments. Previously, we have shown that chiral centers present in either the dimelamine component **1** or the cyanurate component CA quantitatively induce one handedness (*M* or *P*) in the assembly. This offers the possibility to study the amplification of chirality under two different kinetic regimes. When chiral dimelamines **1** are used, the exchange of chiral components and (*M*/*P*)-interconversion, i.e., interconversion between the (*M*)- and (*P*)-isomers of assembly $\mathbf{1}_3\cdot(CA)_6$, take place via identical pathways (condition A). When chiral cyanurates CA are used, the exchange of chiral components occurs much faster than (*M*/*P*)-interconversion (condition B). Experimentally, a much stronger chiral amplification is observed under condition B. For example, the observed chiral amplification for a mixture of chiral and achiral components (40:60) is 46% under condition B and 32% under condition A. Kinetic models were developed to fit the experimental data and to simulate chiral amplification in dynamic systems in general. These simulations show that it is theoretically possible that the diastereomeric excess in a dynamic system is more than 99% with less than 1% chiral component present!

Introduction

Amplification of chirality occurs in systems where a small initial chiral bias induces a high diastereomeric excess (d.e.) or enantiomeric excess (e.e.).[1,2] The main reason for the interest in this phenomenon is its relevance to enantioselective synthesis. Asymmetric autocatalytic reactions and nonlinear effects have been extensively studied to develop systems that display a strong amplification of chirality.[2−5] From a more philosophical point of view it is also regarded essential for the explanation of homochirality in Nature.[6−8] A few years ago, Green and co-workers reported the amplification of chirality in the synthesis of polyisocyanates, having a stiff helical backbone, based on the cooperative action of individual small forces.[9,10] The macromolecular helicity of these polymers can be quantitatively controlled via the incorporation of asymmetric centers in the side chains. They found that the chiroptical properties of the polymer did not change when the ratio of chiral to achiral monomers was lowered from 100:0 to 15:85.[9] Even polymers containing only 0.5% of chiral monomers still expressed a strong chiroptical activity. The reason for this strong amplification is that the achiral components "follow" the helicity induced by the chiral components. This is commonly referred to as the "Sergeants and Soldiers" principle.[9] It is a general phenomenon not restricted to polyisocyanates, but in principle is also applicable to other polymers with stiff helical backbones.[11−15] Chiral amplification has also been observed in noncovalent macromolecular systems.[16,17] Recently, Meijer and co-workers studied the Sergeants and Soldiers principle in dynamic macromolecular aggregates that are held together via noncovalent interactions, such as π-π stacking or hydrogen bonding.[18−20] Large optical activities were observed for chiral columnar assemblies containing only a small fraction (∼5%) of chiral components.[18,21] We have studied the Sergeants and Soldiers principle in dynamic hydrogen-bonded assemblies of well-

* To whom correspondence should be addressed.

† Part of this work has appeared as a preliminary communication.[22]

(1) Green, M. M.; Park, J.-W.; Sato, T.; Teramoto, A.; Lifson, S.; Selinger, R. L. B.; Selinger, J. V. *Angew. Chem.* **1999**, *111*, 3329−3345; *Angew. Chem., Int. Ed. Engl.* **1999**, *38*, 3138−3154.

(2) Feringa, B. L.; Van Delden, R. A. *Angew. Chem.* **1999**, *111*, 3624−3645; *Angew. Chem., Int. Ed. Engl.* **1999**, *38*, 3418−3438.

(3) Kitamura, M.; Suga, S.; Oka, H.; Noyori, R. *J. Am. Chem. Soc.* **1998**, *120*, 9800−9809.

(4) Shibata, T.; Yamamoto, J.; Matsumoto, N.; Yonekubo, S.; Osanai, S.; Soai, K. *J. Am. Chem. Soc.* **1998**, *120*, 12157−12158.

(5) Girard, C.; Kagan, H. *Angew. Chem.* **1998**, *110*, 3088−3127; *Angew. Chem., Int. Ed. Engl.* **1998**, *37*, 2922−2959.

(6) Wald, J. *Ann. N. Y. Acad. Sci.* **1957**, *69*, 353.

(7) Avalos, M.; Babiano, R.; Cintas, P.; Jiménez, J. L.; Palacios, J. C. *Chem. Commun.* **2000**, 887−892.

(8) Buschmann, H.; Thede, R.; Heller, D. *Angew. Chem.* **2000**, *112*, 4197−4200; *Angew. Chem., Int. Ed.* **2000**, *39*, 4033−4035.

(9) Green, M. M.; Rediy, M. P.; Johnson, R. J.; Darling, G.; O'Leary, D. J.; Willson, G. *J. Am. Chem. Soc.* **1989**, *111*, 6452−6454.

(10) Green, M. M.; Peterson, N. C.; Sato, T.; Teramoto, A.; Cook, R.; Lifson, S. *Science* **1995**, *268*, 1860−1866.

(11) Fujiki, M. *J. Am. Chem. Soc.* **1994**, *116*, 11976−11981.

(12) Cornelissen, J. L. M.; Fischer, M.; Sommerdijk, N. A. J. M.; Nolte, R. J. M. *Science* **1998**, *280*, 1427−1430.

(13) Langeveld-Voss, B. M. W.; Waterval, R. J. M.; Janssen, R. A. J.; Meijer, E. W. *Macromolecules* **1999**, *32*, 227−230.

(14) Takei, F.; Onitsuka, K.; Takahashi, S. *Polym. J.* **2000**, *32*, 524−526.

(15) Kozlov, I. A.; Orgel, L. E.; Nielsen, P. E. *Angew. Chem.* **2000**, *112*, 4462−4465; *Angew. Chem., Int. Ed.* **2000**, *39*, 4292−4295.

(16) Yashima, E.; Matsushima, T.; Okamoto, Y. *J. Am. Chem. Soc.* **1997**, *119*, 6345−6359.

(17) Yashima, E.; Maeda, Y.; Okamoto, Y. *J. Am. Chem. Soc.* **1998**, *120*, 8895−8896.

(18) Palmans, A. R. A.; Vekemans, J. A. J. M.; Havinga, E. E.; Meijer, E. W. *Angew. Chem.* **1997**, *109*, 2763−2765; *Angew. Chem., Int. Ed. Engl.* **1997**, *36*, 2648−2651.

(19) Brunsveld, L.; Schenning, A. P. H. J.; Broeren, M. A. C.; Janssen, H. M.; Vekemans, J. A. J. M.; Meijer, E. W. *Chem. Lett.* **2000**, 292−293.

(20) Brunsveld, L.; Lohmeijer, B. G. G.; Vekemans, J. A. J. M.; Meijer, E. W. *Chem. Commun.* **2000**, 2305−2306.

10.1021/ja010610e CCC: $20.00
Published on Web 09/27/2001

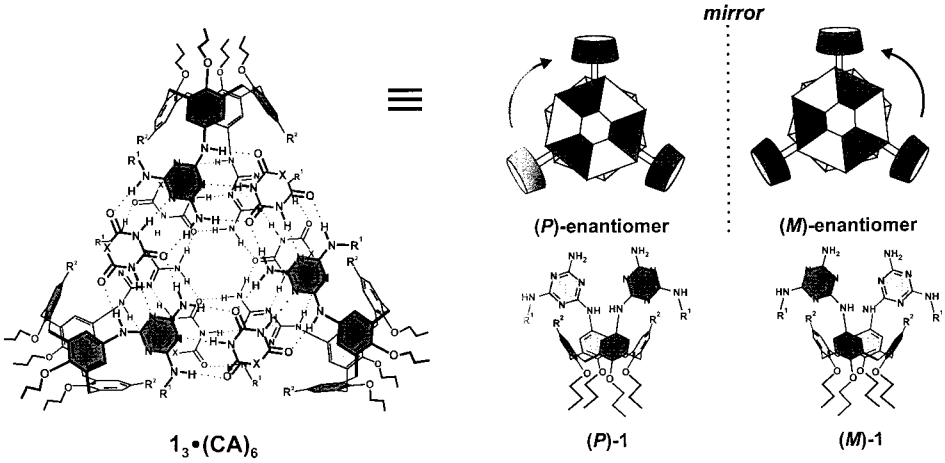

Figure 1. General molecular structure of assemblies $\mathbf{1}_3$•$(CA)_6$ with schematic representations of the (*M*)- and (*P*)-enantiomers. The supramolecular chirality of these assemblies is a result of the staggered orientation of the two melamine fragments of **1**, which can either be positive (*P*) or negative (*M*).

Chart 1

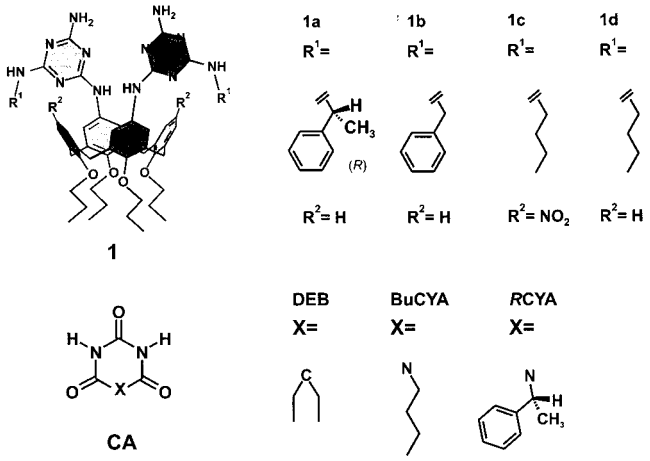

defined molecular composition.[22] Initially, experiments were carried out under thermodynamically controlled conditions. In this paper we describe chiral amplification experiments that are performed under kinetically controlled conditions. These experiments provide remarkable new insights into the application of the Sergeants and Soldiers principle to dynamic systems. Model simulations show that it is possible to obtain a d.e. > 99% in a dynamic system when <1% of the component is chiral.

Results

Hydrogen-bonded assemblies $\mathbf{1}_3$•$(CA)_6$ spontaneously form upon mixing of calix[4]arene dimelamines **1** with barbiturate DEB or cyanurate BuCYA/*R*CYA in a 1:2 ratio in apolar solvents (Chart 1).[23−25] The driving force for the assembly process is the formation of 36 hydrogen bonds between the complementary hydrogen-bonding arrays of the nine components.[26] The assemblies are chiral as a result of a helical twist of the two rosette motifs, which can be either left- (*M*) or right-handed (*P*). The helical twist is caused by a staggered orientation of the two melamine fragments on each calix[4]arene unit (Figure 1). Recently, we found that the enantiomeric assemblies racemize, i.e., interconvert between the (*M*)- and (*P*)-isomers, remarkably slowly (half-life ∼4.5 days at room temperature in benzene).[27] Kinetic studies showed that (*M*/*P*)-interconversion, i.e., interconversion between the (*M*)- and (*P*)-isomers of assembly $\mathbf{1}_3$•$(CA)_6$, requires the complete dissociation of the dimelamine components **1** from the assembly.

In the absence of chiral centers at the periphery, the assemblies form by definition as a racemic mixture of (*M*)- and (*P*)-enantiomers. However, when chiral components are used, the (*M*)- and (*P*)-isomers have a diastereomeric relation and consequently are energetically nondegenerate. Previously, we have shown that the supramolecular chirality of these assemblies can be controlled in a quantitative manner using chiral dimelamines, cyanurates, or barbiturates.[22] For instance, the two (*R*)-1-phenylethylamine moieties present in **1a** induce (*M*)-helicity in assemblies $\mathbf{1a}_3$•$(DEB)_6$ and $\mathbf{1a}_3$•$(BuCYA)_6$ with a d.e. > 98%. This was evidenced by the presence of a single set of ^{1}H NMR signals and a very strong chiroptical activity ($\Delta\epsilon_{max} \approx 100$ L•mol^{-1}•cm^{-1}). In a similar fashion, *R*CYA quantitatively induces (*P*)-helicity in assemblies $\mathbf{1b}_3$•$(RCYA)_6$ and $\mathbf{1c}_3$•$(RCYA)_6$ (d.e. > 98%).

Despite the fact that the double rosette assemblies are thermodynamically stable, their individual components are continuously exchanging. The rate of exchange is primarily dependent on the number and strength of the hydrogen bonds to be broken (12 or 6), which means that the exchange rates of the dimelamines **1** and of the cyanurates/barbiturates CA differ by orders of magnitude.[27] Moreover, the exchange rate of dimelamines is significantly lower when assemblies are formed with cyanurates instead of barbiturates, because of the higher binding strengths of cyanurates.[28,29] Also the solvent polarity and temperature can drastically change the rate of the exchange processes. The slow exchange of the dimelamine components

(21) Van der Schoot, M. M. A. J.; Brunsveld, L.; Sijbesma, R. P.; Ramzi, A. *Langmuir* **2000**, *16*, 10076−10083.
(22) Prins, L. J.; Huskens, J.; De Jong, F.; Timmerman, P.; Reinhoudt, D. N. *Nature* **1999**, *398*, 498−502.
(23) Vreekamp, R. H.; Van Duynhoven, J. P. M.; Hubert, M.; Verboom, W.; Reinhoudt, D. N. *Angew. Chem.* **1996**, *108*, 1306−1309; *Angew. Chem. Int. Ed. Engl.* **1996**, *35*, 1215−1218.
(24) Timmerman, P.; Vreekamp, R. H.; Hulst, R.; Verboom, W.; Reinhoudt, D. N.; Rissanen, K.; Udachin, K. A.; Ripmeester, J. *Chem.*−*Eur. J.* **1997**, *3*, 1823−1832.
(25) Prins, L. J.; Jolliffe, K. A.; Hulst, R.; Timmerman, P.; Reinhoudt, D. N. *J. Am. Chem. Soc.* **2000**, *122*, 3617−3627.
(26) Whitesides, G. M.; Simanek, E. E.; Mathias, J. P.; Seto, C. T.; Chin, D. N.; Mammen, M.; Gordon, D. M. *Acc. Chem. Res.* **1995**, *28*, 37−44.
(27) Prins, L. J.; De Jong, F.; Timmerman, P.; Reinhoudt, D. N. *Nature* **2000**, *408*, 181−184.
(28) Shieh, H. S.; Voet, D. *Acta Crystallogr., Sect. B: Struct. Sci.* **1976**, *32*, 3254−3260.
(29) Mascal, M.; Fallon, P. S.; Batsanov, A. S.; Heywood, B. R.; Champ, S.; Colclough, M. *Chem. Commun.* **1995**, 805−806.

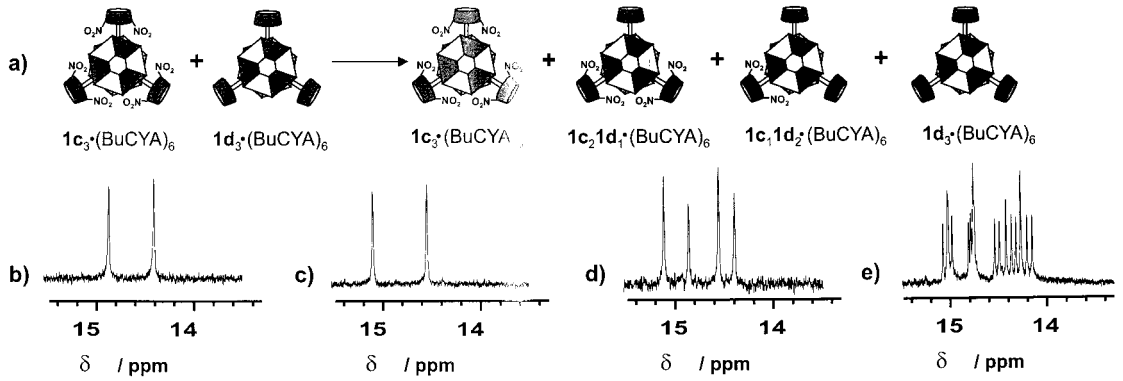

Figure 2. (a) Mixing homomeric assemblies $\mathbf{1c}_3$•(BuCYA)$_6$ and $\mathbf{1d}_3$•(BuCYA)$_6$ results in the formation of heteromeric assemblies $\mathbf{1c}_2\mathbf{1d}_1$•(BuCYA)$_6$ and $\mathbf{1c}_1\mathbf{1d}_2$•(BuCYA)$_6$ because of an exchange of calix[4]arene dimelamines **1c** and **1d**. Part of the ^{1}H NMR spectra of (b) $\mathbf{1c}_3$•(BuCYA)$_6$, (c) $\mathbf{1d}_3$•(BuCYA)$_6$, and (d) a 1:1 mixture of $\mathbf{1c}_3$•(BuCYA)$_6$ and $\mathbf{1d}_3$•(BuCYA)$_6$ recorded immediately after mixing. (e) The same mixture after heating for 3 h at 70 °C. All spectra were recorded in benzene-d_6 at 70 °C.

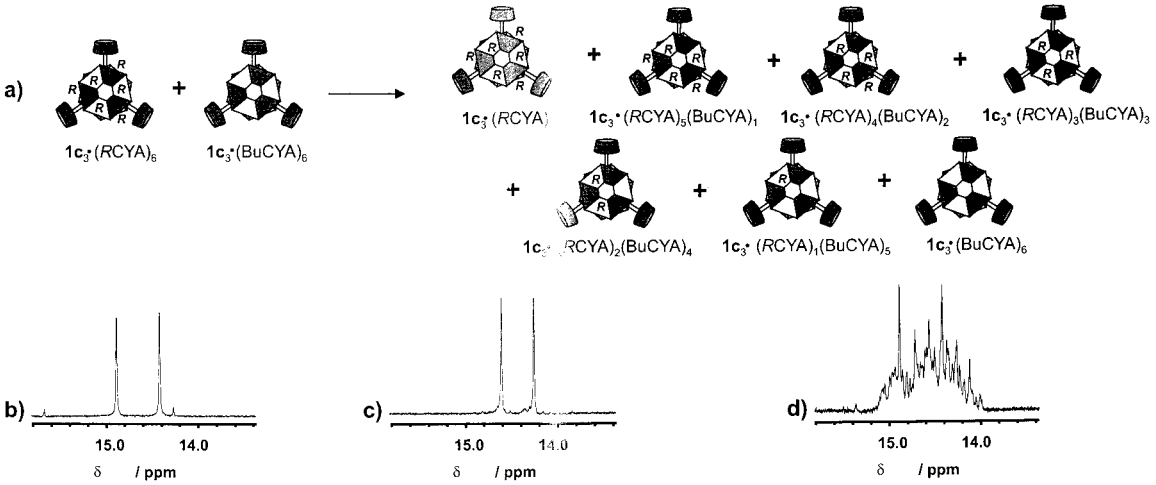

Figure 3. (a) Mixing homomeric assemblies $\mathbf{1c}_3$•(*R*CYA)$_6$ and $\mathbf{1c}_3$•(BuCYA)$_6$ results in the formation of heteromeric assemblies $\mathbf{1c}_3$•(*R*CYA)$_n$(BuCYA)$_{6-n}$ ($n = 1-5$) because of an exchange of *R*CYA and BuCYA. Part of the ^{1}H NMR spectra of (b) $\mathbf{1c}_3$•(BuCYA)$_6$, (c) $\mathbf{1c}_3$•(*R*CYA)$_6$, and (d) a 1:1 mixture of $\mathbf{1c}_3$•(*R*CYA)$_6$ and $\mathbf{1c}_3$•(BuCYA)$_6$ recorded 15 min after mixing. All spectra were recorded in benzene-d_6 at room temperature.

1 in benzene-d_6 *at 70 °C* is illustrated by the fact that the ^{1}H NMR spectrum recorded immediately after homomeric assemblies $\mathbf{1c}_3$•(BuCYA)$_6$ and $\mathbf{1d}_3$•(BuCYA)$_6$ were mixed did not show any signals corresponding to the heteromeric assemblies $\mathbf{1c}_n\mathbf{1d}_{3-n}$•(BuCYA)$_6$ ($n = 1$, 2) (Figure 2a,d). Only after prolonged heating, new signals originating from the heteromeric assemblies appear slowly. Extrapolation using model calculations showed that it takes 10 h at 70 °C before the thermodynamic equilibrium is reached (Figure 2e). From these ^{1}H NMR measurements a rate constant of $(7.0 \pm 0.4) \times 10^{-5}$ s^{-1} was determined for the exchange of dimelamines **1c** and **1d** in benzene-d_6 at 70 °C. The cyanurate assemblies used in this study, i.e., $\mathbf{1a}_3$•(BuCYA)$_6$ and $\mathbf{1b}_3$•(BuCYA)$_6$, behave similarly.

The exchange of cyanurate components is fast under the same conditions. Mixing of homomeric assemblies $\mathbf{1c}_3$•(*R*CYA)$_6$ and $\mathbf{1c}_3$•(BuCYA)$_6$ in a 1:1 ratio in benzene-d_6 results in the formation of the heteromeric assemblies $\mathbf{1c}_3$•(*R*CYA)$_n$(BuCYA)$_{6-n}$ ($n = 1-5$) via an exchange of cyanurates *R*CYA and BuCYA. The ^{1}H NMR spectrum recorded *at room temperature* immediately after mixing showed the presence of numerous new signals originating from the assemblies $\mathbf{1c}_3$•(*R*CYA)$_n$(BuCYA)$_{6-n}$ ($n = 1-5$) (Figure 3d). The much faster exchange rate of cyanurates compared to dimelamines is not surprising, since only six H-bonds need to be broken to expel a cyanurate component from the assembly.

Chiral Amplification under Thermodynamically Controlled Conditons: The Sergeants and Soldiers Principle. Mixing of solutions of assembly (*M*)-$\mathbf{1a}_3$•(DEB)$_6$ and racemic assembly $\mathbf{1b}_3$•(DEB)$_6$ results in the formation of the heteromeric assemblies $\mathbf{1a}_2\mathbf{1b}_1$•(DEB)$_6$ and $\mathbf{1a}_1\mathbf{1b}_2$•(DEB)$_6$ (Figure 4a−c).[22,30] In this case the thermodynamic equilibrium is reached within seconds after mixing, which is much faster than the assemblies comprising BuCYA. This is caused by the high exchange rate of dimelamines **1a** and **1b** in the less stable barbiturate assemblies and the solvent chloroform. NMR analysis using a variety of 2D techniques has previously shown that for this type of assembly the distribution of components **1a** and **1b** over the four assemblies is nearly statistical.[30]

Interestingly, we found that the CD intensities of mixtures of (*M*)-$\mathbf{1a}_3$•(DEB)$_6$ and $\mathbf{1b}_3$•(DEB)$_6$ were significantly higher than the sum of the CD intensities of the individual assemblies (corrected for the relative ratio **1a:1b**; see Figure 4d). This phenomenon, which has also been observed in other dynamic systems,[16−20] is an example of chiral amplification. It is directly related to the presence of the heteromeric assemblies $\mathbf{1a}_2\mathbf{1b}_1$•(DEB)$_6$ and $\mathbf{1a}_1\mathbf{1b}_2$•(DEB)$_6$. These assemblies contain four or two (*R*)-substituents, respectively, and this leads to the preferential formation of the corresponding (*M*)-diastereomers. Ap-

(30) Crego Calama, M.; Fokkens, R.; Nibbering, N. M. M.; Timmerman, P.; Reinhoudt, D. N. *Chem. Commun.* **1998**, 1021−1022.

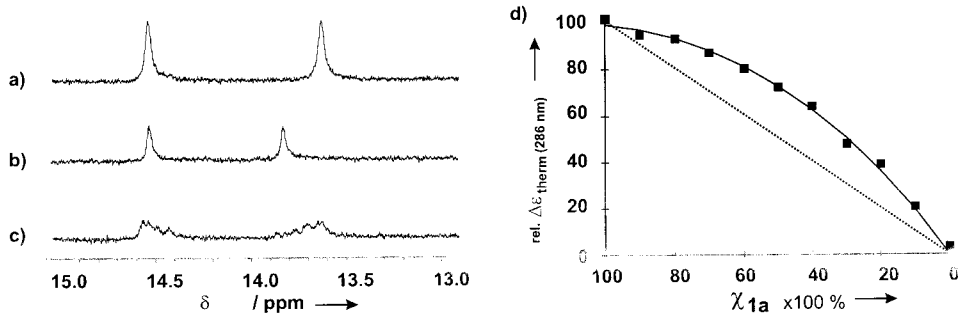

Figure 4. Part of the ^{1}H NMR spectra of (a) **1a**$_3$·(DEB)$_6$, (b) **1b**$_3$·(DEB)$_6$, and (c) a 1:1 mixture of **1a**$_3$·(DEB)$_6$ and **1b**$_3$·(DEB)$_6$. The spectra were recorded in $CDCl_3$ at room temperature immediately after mixing. (d) Relative CD intensity (filled squares, measured at 286 nm) versus the mole fraction of chiral component **1a**, measured in chloroform at room temperature. The line represents the calculated best fit for $\Delta H^\circ_{tot} = -13.4$ kJ·mol^{-1}.

parently, the d.e. for these assemblies is significantly higher than 66% (**1a**$_2$**1b**$_1$·(DEB)$_6$) or 33% (**1a**$_1$**1b**$_2$·(DEB)$_6$), values expected when the d.e. is related in a linear fashion to the number of chiral centers present. This is the phenomenon described by Green and co-workers as the Sergeants and Soldiers principle, which indicates that within the assembly the achiral units follow the helicity induced by the chiral units.[9]

As a first step, the nonlinear CD curve was fitted to a simple model based on an enthalpy difference, $\Delta H^\circ_{M/P}$, between the (*M*)- and (*P*)-diastereomers of assemblies **1a**$_n$**1b**$_{3-n}$·(DEB)$_6$ ($n = 1-3$) at thermodynamic equilibrium.[22] The entropy term ΔS° was considered to be equal for all assemblies, since they all comprise nine components and have similar structures. Cooperativity between chiral centers was not included in the model, and therefore $\Delta H^\circ_{M/P}$ was assumed to increase linearly with the number of chiral substituents present. Linear regression analysis of the CD data resulted in $\Delta H^\circ_{M/P}$(298 K) = 2.23 kJ·mol^{-1} per chiral substituent. This corresponds to an enthalpy difference ΔH°_{tot}(298 K) = 13.4 kJ·mol^{-1} between the (*M*)- and (*P*)-diastereomers of assembly **1a**$_3$·(DEB)$_6$, which contains six chiral substituents.

Chiral Amplification under Kinetically Controlled Conditions. Subsequently, we have investigated chiral amplification in assemblies **1**$_3$·(CA)$_6$ under conditions at which the exchange of the dimelamine components **1** is slow on the laboratory time scale (referred to as "chiral amplification under kinetic control"). We have performed two different sets of experiments. First, we have studied chiral amplification in mixtures of assemblies **1a**$_n$**1b**$_{3-n}$·(BuCYA)$_6$ ($n = 0-3$) containing both chiral and achiral dimelamines. In this case both the exchange of chiral and achiral components **1** and the (*M*/*P*)-interconversion occur via the same pathway, and consequently these processes have identical rates. Second, we have studied mixtures of assemblies **1c**$_3$·(*R*CYA)$_n$(BuCYA)$_{6-n}$ ($n = 0-6$) containing both chiral and achiral cyanurates. In these experiments, the exchange of chiral and achiral components CA and the (*M*/*P*)-interconversion occur via different pathways with a much lower rate for the (*M*/*P*)-interconversion.

Mixing Chiral and Achiral Dimelamines (Experiments A). In these experiments induction of chirality in double rosette assemblies **1a**$_n$**1b**$_{3-n}$·(BuCYA)$_6$ ($n = 0-3$) occurs via the (*R*)-phenylethyl substituents in dimelamine **1a**. Solutions of assemblies (*M*)-**1a**$_3$·(BuCYA)$_6$ and racemic **1b**$_3$·(BuCYA)$_6$ in benzene (1.0 mM) were mixed in ratios ranging from 90:10 to 10:90, and the CD intensity at 305 nm was measured as a function of time at 70 °C. From these measurements the relative CD intensities compared to the CD intensity of a 1.0 mM solution of (*M*)-**1a**$_3$·(BuCYA)$_6$ were determined and plotted as a function of time (Figure 5a). It was assumed that all assemblies present have the same $\Delta\epsilon_{305}$, which seems reasonable regarding their very similar molecular structures.[31] Figure 5a shows that the relative CD intensities at $t = 0$ correspond to the initial mole fraction of (*M*)-**1a**$_3$·(BuCYA)$_6$ present. However, the CD intensities increase over time as a result of the formation of the heteromeric assemblies **1a**$_2$**1b**$_1$·(BuCYA)$_6$ and **1a**$_1$**1b**$_2$·(BuCYA)$_6$ (vide supra). After approximately 3 h constant values for $\Delta\epsilon_{305}$ are reached. In the remainder of the text, these thermodynamic values will be referred to as $\Delta\epsilon_{therm}$ (for simulations d.e.$_{therm}$).[32] A plot of $\Delta\epsilon_{therm}$ as a function of the ratio **1a**:**1b** shows the typical nonlinear behavior of a Sergeants and Soldiers experiment (Figure 5c).

Mixing Chiral and Achiral Cyanurates (Experiments B). In experiments B chiral induction in double rosette assemblies **1c**$_3$·(*R*CYA)$_n$(BuCYA)$_{6-n}$ ($n = 0-6$) occurs via the (*R*)-phenylethyl substituents in *R*CYA. Solutions of assemblies (*P*)-**1c**$_3$·(*R*CYA)$_6$ and racemic **1c**$_3$·(BuCYA)$_6$ in benzene (1.0 mM) were mixed in ratios varying between 90:10 and 10:90 at 70 °C, and the CD intensity at 308 nm was measured as a function of time. The $\Delta\epsilon_{308}$ value of assembly **1c**$_3$·(BuCYA)$_6$ (−73.8 L·mol^{-1}·cm^{-1})[27] is significantly lower than the $\Delta\epsilon_{308}$ value of assembly (*P*)-**1c**$_3$·(*R*CYA)$_6$ (−103.8 L·mol^{-1}·cm^{-1}), because of the absence of six benzyl chromophores. The measured CD intensities were related to a calculated 100% value for the mixture based on the ratio **1c**$_3$·(*R*CYA)$_6$:**1c**$_3$·(BuCYA)$_6$ (Figure 5b).[33] For example, the 100% value for a 40:60 mixture of **1c**$_3$·(*R*CYA)$_6$ and **1c**$_3$·(BuCYA)$_6$ was calculated to be −85.8 L·mol^{-1}·cm^{-1}. The CD intensities increase rapidly in time, particularly for high ratios of *R*CYA/BuCYA. As a result, the relative CD intensities at $t = 0$ do not correspond in all cases to the initial mole fraction of (*M*)-**1a**$_3$·(BuCYA)$_6$. In all cases $\Delta\epsilon_{therm}$ is reached after approximately 30 min (Figure 5c).

Comparison of the Results of Experiments A and B. Although both experiments at first sight seem very similar, there are some remarkable differences, both in the time scale at which chiral amplification takes place and in the $\Delta\epsilon_{therm}$ values. First, the time at which $\Delta\epsilon$ starts to change (t_{init}) is about 100 s in experiment A, whereas the $\Delta\epsilon$ in experiment B increases immediately after mixing ($t_{init} = 0$). Second, t_{init} in experiment

(31) Previous studies have shown that assemblies containing similar chromophores exhibit similar CD intensities.

(32) Defined as d.e.$_{therm}$ = ([*M*]$_{therm}$ − [*P*]$_{therm}$)/([*M*]$_{therm}$ + [*P*]$_{therm}$); $\Delta\epsilon_{therm} = \Delta\epsilon_{therm,M} - \Delta\epsilon_{therm,P}$.

(33) It is assumed that the CD intensity of heteromeric assemblies **1c**$_3$·(*R*CYA)$_n$(BuCYA)$_{6-n}$ ($n = 1-5$) is linearly composed of the CD intensities of the homomeric assemblies **1c**$_3$·(*R*CYA)$_6$ and **1c**$_3$·(BuCYA)$_6$. In reality, this is not necessarily true as a result of slightly different orientations of the chromophores in the heteromeric assemblies compared to the homomeric assemblies. This might explain why the values for high ratios of *R*CYA to BuCYA are slightly higher than 100%.

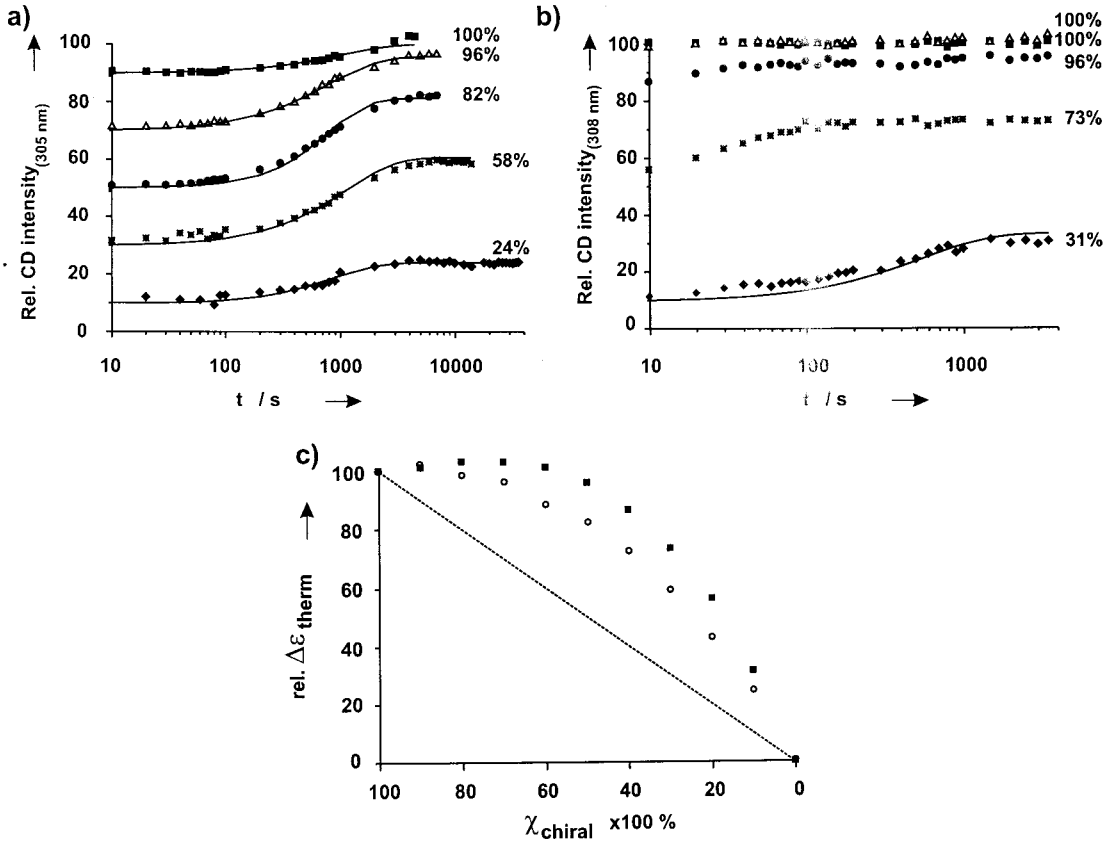

Figure 5. (a) Increase of the relative CD intensity (at 305 nm) in time for mixtures of (*M*)-**1a**$_3$·(BuCYA)$_6$ and **1b**$_3$·(BuCYA)$_6$ with different initial mole fractions of (*M*)-**1**$_3$·(BuCYA)$_6$ (■, 90%; △, 70%; ●, 50%; *, 30%; ◆, 10%). All spectra were measured in benzene at 70 °C. The solid lines represent the best fits using model A. (b) Increase of the relative CD intensity (at 308 nm) in time for mixtures of (*P*)-**1c**$_3$·(*R*CYA)$_6$ and **1c**$_3$·(BuCYA)$_6$ with different initial mole fractions of (*P*)-**1c**$_3$·(*R*CYA)$_6$ (■, 90%; △, 70%; ●, 50%; *, 30%; ◆, 10%). The solid line represents the best fit to model B. All measurements were performed in benzene at 70 °C. (c) Relative CD intensities at the thermodynamic equilibrium obtained in experiments A (○) and B (■) for different mole fractions of chiral component (**1a** in experiment A and *R*CYA in experiment B).

A is virtually independent of the ratio **1a**:**1b**, while in experiment B t_{init} depends strongly on the ratio *R*CYA:BuCYA. For example, when *R*CYA and BuCYA are present in a ratio of 90:10 or 70:30 induction is so fast that intermediate values for $\Delta\epsilon_{therm}$ are not measurable. At *R*CYA:BuCYA = 10:90 t_{init} is about 100 s and roughly equals t_{init} in experiment A. Finally, significantly higher $\Delta\epsilon_{therm}$ values are obtained in experiment B compared to experiment A for the same ratio of chiral and achiral components (Figure 5c). For example, $\Delta\epsilon_{therm}$ = 86% in experiment B for a ratio of *R*CYA to BuCYA of 40:60, whereas $\Delta\epsilon_{therm}$ is only 72% for the same ratio of chiral to achiral components in experiment A.[34] To explain the observed differences, we developed theoretical models A and B that describe the essential kinetic processes that take place in both experiments. These models will be discussed first.

Kinetic Models for Chiral Amplication in Double Rosette Assemblies. *Model A.* Model A describes all relevant dissociations and associations that occur in a mixture of assemblies (M)-**1a**$_3$·(BuCYA)$_6$ and **1b**$_3$·(BuCYA)$_6$ (experiment A). The mixture is treated as an equilibrating system containing eight different assemblies, three intermediate assemblies, and the free components **1a** and **1b** (Figure 6). The model considers the (*M*)- and (*P*)-diastereomers of the homomeric assemblies **1a**$_3$·(BuCYA)$_6$ and **1b**$_3$·(Bu(CYA)$_6$ and the heteromeric assemblies **1a**$_2$**1b**$_1$·(BuCYA)$_6$ and **1a**$_1$**1b**$_2$·(BuCYA)$_6$. These assemblies are all in equilibrium with the intermediate assemblies **1a**$_2$·(BuCYA)$_6$, **1a**$_1$**1b**$_1$·(BuCYA)$_6$, and **1b**$_2$·(BuCYA)$_6$, obtained after dissociation of one dimelamine component. Previous studies have shown that assembly formation is highly cooperative, and for this reason the dissociation of the first dimelamine **1** from an assembly is considered to be the rate-determining step.[27] For this reason, further dissociation of the intermediate assemblies is consequently not incorporated into the model. It is important to notice that dissociation of either a (*P*)- or an (*M*)-assembly results in a loss of the supramolecular chirality. Therefore, intermediate assemblies **1a**$_2$·(BuCYA)$_6$, **1a**$_1$**1b**$_1$·(BuCYA)$_6$, and **1b**$_2$·(BuCYA)$_6$ are treated as *achiral* species. Consistent with previously obtained experimental data, interconversion between the (*M*)- and (*P*)-assemblies requires dissociation of the assembly.[27] This means that the exchange of dimelamines and (*M*/*P*)-interconversion occur via identical pathways.

The difference in free energy between diastereomeric assemblies, the origin of chiral induction, is reflected by a lower kinetic stability of the thermodynamically unfavorable (*P*)-diastereomers. To account for this difference, we have introduced a factor f_m for each chiral center present that increases the dissociation rate of dimelamines **1** from the (*P*)-diastereomers compared to the (*M*)-diastereomer.[35] For example, the dissociation rate of dimelamines **1a** and **1b** from assembly

(34) These values correspond to a chiral amplification of 46% and 32%, respectively.

(35) In principle, the different thermodynamic stabilities of the diastereomeric assemblies (*M*)-**1a**$_n$**1b**$_{3-n}$·(BuCYA)$_6$ (n = 3−1) and (*P*)-**1a**$_n$**1b**$_{3-n}$·(BuCYA)$_6$ (n = 3−1) could be reflected by both different association and different dissociation rates of dimelamines **1** from the respective assemblies. However, it is assumed that the differences in the association rates are not relevant because the time scale at which chiral amplification takes place is determined by the rate-determing step (i.e., $k_{dis,m}$).

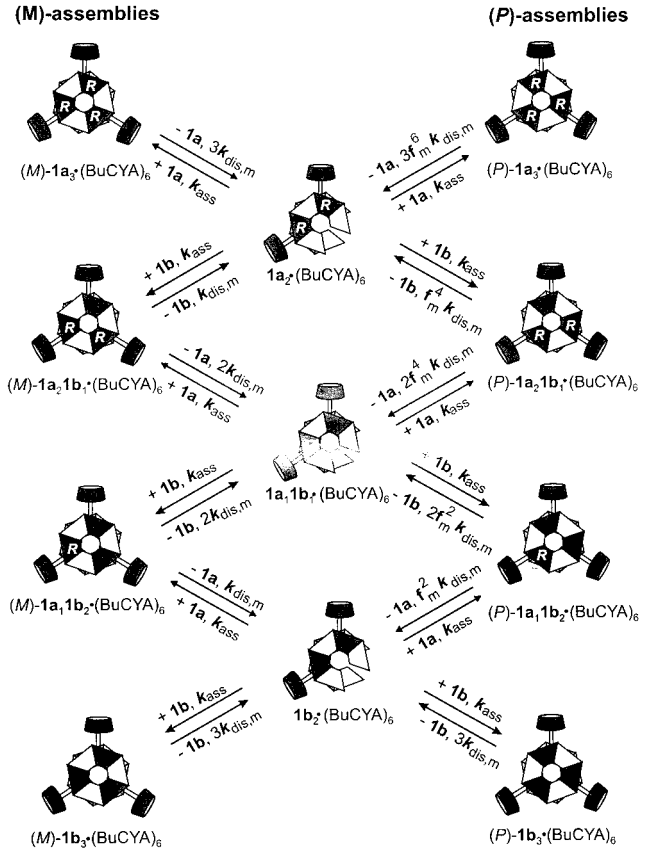

Figure 6. Kinetic model A describing the relevant exchange and interconversion processes that occur in a mixture of assemblies (*M*)-**1a**$_3$•(BuCYA)$_6$ and **1b**$_3$•(BuCYA)$_6$.

(*P*)-**1a**$_2$**1b**$_1$•(BuCYA)$_6$ is a factor f_m^4 higher than from (*M*)-**1a**$_2$**1b**$_1$•(BuCYA)$_6$, because of the presence of four chiral centers. The increase in f_m is consistent with the linear increase in $\Delta H^\circ_{M/P}$ previously used in our thermodynamic model ($f_m = e^{-\Delta G^\circ_{M/P}/RT}$).[22,36] Also here, cooperativity between the chiral centers is not included in the model. All association steps are equal and are considered to be fast ($k_{ass} = 10^5$ L•mol^{-1}•s^{-1}, vide infra). For the dissociation steps statistical factors are introduced to account for all different possibilities of dissociation. The exchange of BuCYA is not incorporated into model A, since it is assumed to be fast for all assemblies and considered not to influence the chiral amplification of the system.

Model B. Model B describes all relevant dissociations and associations that occur in a mixture of assemblies (P)-**1c**$_3$•(RCYA)$_6$ and **1c**$_3$•(BuCYA)$_6$ (experiment B). Model B is more extended than model A, because of the increased number of heteromeric assemblies present (Figure 7). Furthermore, the exchange of cyanurates is included, since the chiral centers reside on these components. As in model A, (*M*/*P*)-interconversion occurs via intermediate achiral assemblies **1c**$_2$•(*R*CYA)$_n$(BuCYA)$_{6-n}$ ($n = 0-6$), obtained after dissociation of **1c** from assemblies **1c**$_3$•(*R*CYA)$_n$(BuCYA)$_{6-n}$ ($n = 0-6$). Exchange of *R*CYA and BuCYA occurs via intermediate assemblies (*M*)-**1c**$_3$•(*R*CYA)$_n$(BuCYA)$_{5-n}$ ($n = 0-5$) and (*P*)-**1c**$_3$•(*R*CYA)$_n$(BuCYA)$_{5-n}$ ($n = 0-5$). It is assumed that the exchange of cyanurates occurs independently from the exchange of dimelamines and does not affect the chirality of the assemblies. Again, the parameter f_m is used to account for the difference in kinetic stability between the (*M*)- and (*P*)-diastereomers, the latter being more stable when *R*CYA is used. The dissociation rates of both *R*CYA and BuCYA are regarded to be equal for all assemblies. Despite the fact that this assumption is not completely valid (discussion below), it seems unlikely that the small difference in exchange rates will influence the chiral amplification. All association constants, for both dimelamines and cyanurates, are considered to be fast ($k_{ass,m} = k_{ass,c} = 10^5$ L•mol^{-1}•s^{-1}). As in model A, statistical factors are introduced to account for the different possibilities of dissociation.

Simulations Using Theoretical Models A and B. To understand how the different parameters in models A and B affect the chiral amplification, a number of simulations were performed in which the initial ratio of chiral and achiral components, f_m, $k_{dis,m}$, $k_{ass,m}$, and $k_{ass,c}$ were systematically varied over a wide range of different values.

Initial Ratio of Chiral to Achiral Components. The initial ratios of (*M*)-**1a**$_3$•(BuCYA)$_6$/**1b**$_3$•(BuCYA)$_6$ and (*P*)-**1c**$_3$•(*R*CYA)$_6$/**1c**$_3$•(BuCYA)$_6$ in models A and B, respectively, were systematically varied between 90:10 and 10:90 with constant values of $k_{dis,m} = 10^{-5}$ s^{-1} and $f_m = 2$ ($k_{dis,c} = 0.1$ s^{-1} in model B). The value for $k_{dis,m}$ is based on previously obtained experimental data for this type of assembly.[27] The resulting plots of the calculated d.e. as a function of time are depicted in Figure 8a,b.

The three experimentally observed differences between experiments A and B (vide supra) are clearly recognizable in these simulations. For model A, t_{init} is identical ($\sim 10^4$ s) for all ratios **1a**/:**1b** (Figure 8a). For model B, t_{init} is dependent on the ratio *R*CYA/BuCYA, but is for all ratios of *R*CYA to BuCYA smaller than the t_{init} value of 10^4 s in model A (Figure 8b). Finally, the calculated d.e.$_{therm}$ values are much higher for model B than for model A (Figure 8c).

Parameter f_m. In both models parameter f_m is used to create a difference in stability between the (*M*)- and (*P*)-diastereomers. Each chiral substituent present in the unfavorable isomer increases the dissociation rate of the dimelamine components **1** with a factor $f_m = e^{-\Delta G^\circ_{M/P}/RT}$. The influence of f_m was studied by systematically varying the parameter between 1 and 10 for a constant ratio chiral:achiral = 40:60 and $k_{dis,m} = 10^{-5}$ s^{-1} ($k_{dis,c} = 0.1$ s^{-1}). The plots of the calculated d.e. as a function of time using models A and B are depicted in parts a and c, respectively, of Figure 9.

When $f_m = 1$, all (*M*)- and (*P*)-assemblies are equal in stability and have identical dissociation rates for the dimelamines **1**. Consequently, this results in d.e.$_{therm}$ = 0% for both models with a distribution of assemblies **1a**$_n$**1b**$_{3-n}$•(BuCYA)$_6$ ($n = 0-3$) and **1c**$_3$•(*R*CYA)$_n$(BuCYA)$_{6-n}$ ($n = 0-6$) entirely determined by statistics. As expected, d.e.$_{therm}$ increases when $f_m > 1$, but the maximum values that can be obtained in both models are very different. Using model A, the d.e.$_{therm}$ does not exceed 73% (Figure 9b), whereas for model B values higher than 99% can be obtained (Figure 9d). This is further exemplified by calculations of the maximum values of d.e.$_{therm}$ for all ratios chiral:achiral with $f_m = 100$ (Figure 8d). From these calculations it can be concluded that the chirality can be quantitatively amplified *for all ratios chiral:achiral* using model B.

Parameter $k_{dis,m}$. The parameter $k_{dis,m}$ was systematically varied between 10^{-1} and 10^{-7} s^{-1} with a constant ratio of chiral to achiral of 40:60 and $f_m = 2$ ($k_{dis,c} = 0.1$ s^{-1} in model B). Plots of the calculated d.e. values as a function of time using models A and B are depicted in Figure 10a,b. In model A the parameter $k_{dis,m}$ only determines t_{init} and has no effect on d.e.$_{therm}$

(36) In contrast to the thermodynamic model, the entropy terms are not equal for all assemblies in the kinetic models A and B (eight or nine components). Therefore, the different stabilities of the (*M*)- and (*P*)-diastereomers in these models are interpreted in terms of a free energy difference $\Delta G^\circ_{M/P}$.

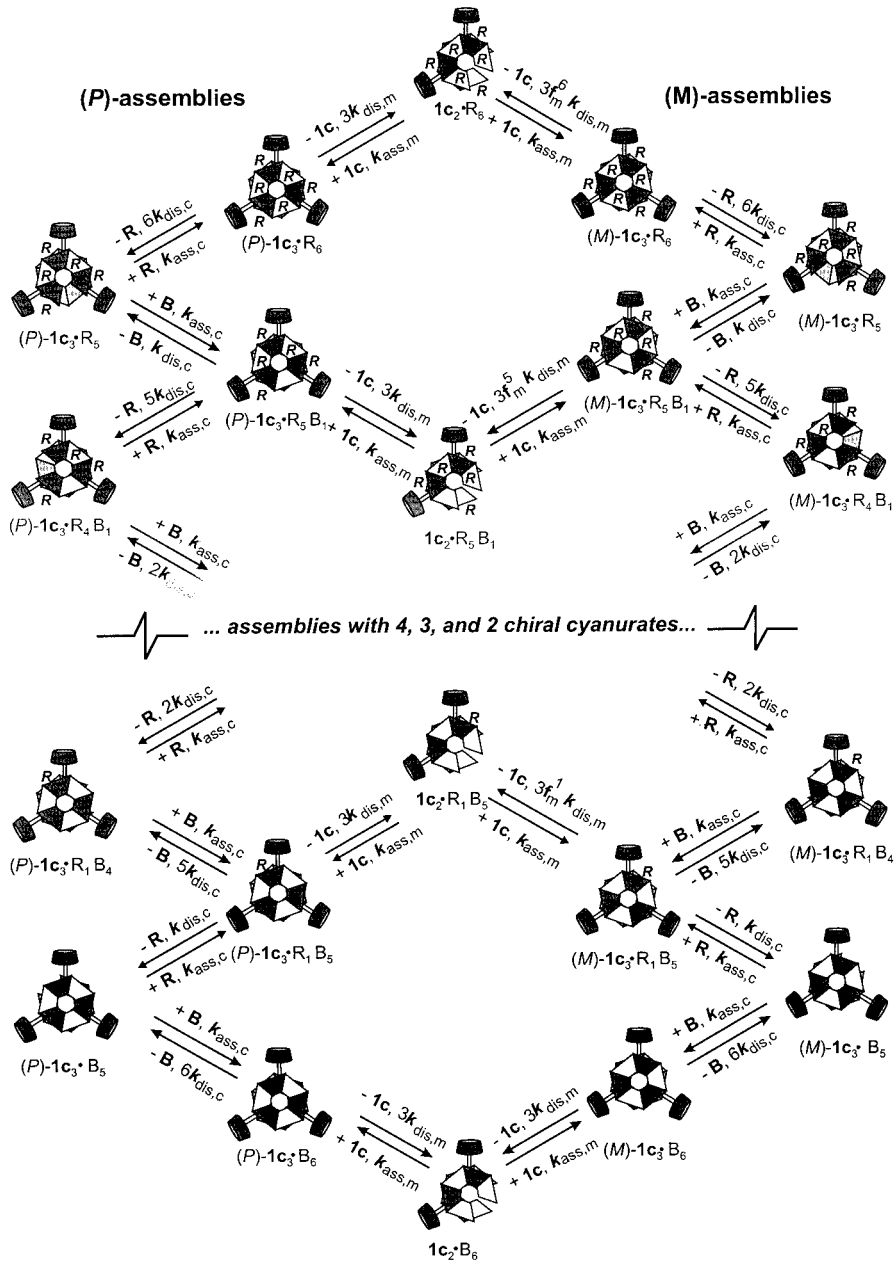

Figure 7. Kinetic model B describing the relevant exchange and interconversion processes that occur in a mixture of assemblies (*P*)-**1c**$_3$·(*R*CYA)$_6$ (i.e., (*P*)-**1c**$_3$·R$_6$) and **1c**$_3$·(BuCYA)$_6$ (i.e.**, 1c**$_3$·B$_6$). For clarity reasons the assemblies containing four, three, and two chiral cyanurates (**1c**$_3$·R$_4$B$_2$, **1c**$_3$·R$_3$B$_3$, and **1c**$_3$·R$_2$B$_4$) and their intermediates are not shown.

at all. On the other hand, in model B $k_{dis,m}$ influences both t_{init} and d.e.$_{therm}$. For high values of $k_{dis,m}$ (10^{-1}−10^{-2} s^{-1}) t_{init} is smaller than for low values (10^{-5}−10^{-7} s^{-1}), but surprisingly this results also in much lower d.e.$_{therm}$ values (64% versus 76%).

Parameter $k_{dis,c}$. In model B, the parameter $k_{dis,c}$ was varied between 10^{1} and 10^{-7} s^{-1} for constant values of $k_{dis,m} = 10^{-5}$ s^{-1} and (*P*)-**1c**$_3$·(*R*CYA)$_6$:**1c**$_3$·(BuCYA)$_6$ = 40:60. Although in reality not possible, simulations were performed with $k_{dis,c} = 10^{-6}$ and 10^{-7} s^{-1} to simulate what happens if the cyanurate exchange is slower than the dimelamine exchange. A plot of d.e.$_{therm}$ as a function of $k_{dis,c}$ is given in Figure 11. For $k_{dis,c}$ values higher than 10^{-3} s^{-1} the d.e.$_{therm}$ is constant at 76.5%. The calculated d.e.$_{therm}$ decreases when $k_{dis,c}$ is only 1−100× higher than $k_{dis,m}$ (10^{-3}−10^{-5} s^{-1}). When $k_{dis,c} < k_{dis,m}$, the d.e.$_{therm}$ remains again constant at 62.5%.

Parameters $k_{ass,c}$ and $k_{ass,m}$. Changing either parameter $k_{ass,c}$ or $k_{ass,m}$ between 10^{2} and 10^{10} L·mol^{-1}·s^{-1} has no effect on the simulations. Values lower than 10^{2} L·mol^{-1}·s^{-1} are not realistic.

Discussion of the Simulations

The Value of t_{init}. The simulations using model A (Figure 8a) show that after mixing of the homomeric assemblies it takes ∼10^{4} s (t_{init}) before the d.e. starts to increase.[37] Furthermore, t_{init} is the same for all ratios **1a**:**1b**. This is rationalized by the fact that an increase in d.e. requires the presence of heteromeric assemblies **1a**$_2$**1b**$_1$·(BuCYA)$_6$ and **1a**$_1$**1b**$_2$·(BuCYA)$_6$ (vide supra). In model A these assemblies can only form *after* dissociation of dimelamines **1a** and **1b** from the homomeric assemblies (*M*)-**1a**$_3$·(BuCYA)$_6$ and **1b**$_3$·(BuCYA)$_6$. Since these

(37) Initially a small decrease in d.e. is observed. This is caused by the fact that assembly (*M*)-**1a**$_3$·(BuCYA)$_6$ (d.e. = 100%) dissociates to form intermediate **1a**$_2$·(BuCYA)$_6$, which is achiral. This intermediate rapidly forms both the (*M*)- and (*P*)-diastereomers of **1a**$_2$**1b**$_1$·(BuCYA)$_6$ *in equal amounts*, since k_{ass} is the same for both diastereomers. At this time scale both diastereomers are kinetically stable, and as a result the d.e. decreases. In time the thermodynamic equilibrium is reached, and the difference in kinetic stability of the (*M*)- and (*P*)-diastereomers is fully reflected by d.e.$_{therm}$.

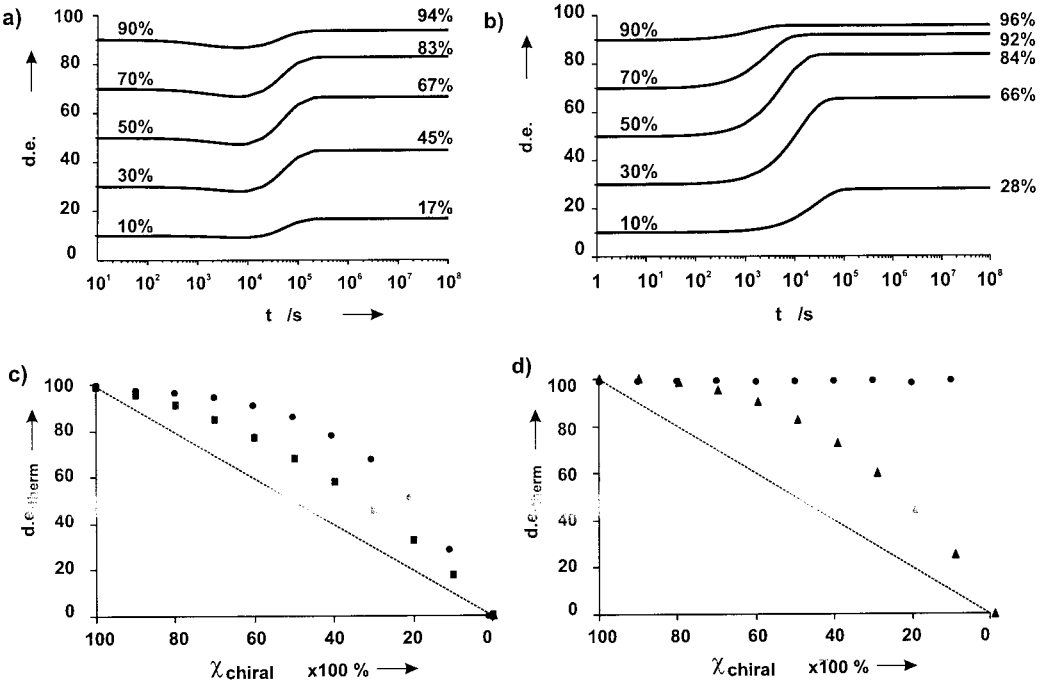

Figure 8. (a) Calculated d.e. as a function of time using model A for different initial mole fractions of (*M*)-rosette (90%, 70%, 50%, 30%, and 10%) with $k_{dis,m} = 10^{-5}$ s^{-1} and $f_m = 2$. (b) Calculated d.e. as a function of time using model B for different initial mole fractions of (*P*)-rosette (90%, 70%, 50%, 30%, and 10%) with $k_{dis,m} = 10^{-5}$ s^{-1}, $k_{dis,c} = 0.1$ s^{-1}, and $f_m = 2$. (c) d.e.$_{therm}$ values using models A (■) and B (●) as a function of the mole fraction of chiral component with $k_{dis,m} = 10^{-5}$ s^{-1} , $k_{dis,c} = 0.1$ s^{-1}, and $f_m = 2$. (d) *Maximum* d.e.$_{therm}$ values that can be obtained using models A (▲) and B (●) as a function of the mole fraction of chiral component with $k_{dis,m} = 10^{-5}$ s^{-1} , $k_{dis,c} = 0.1$ s^{-1}, and $f_m = 100$.

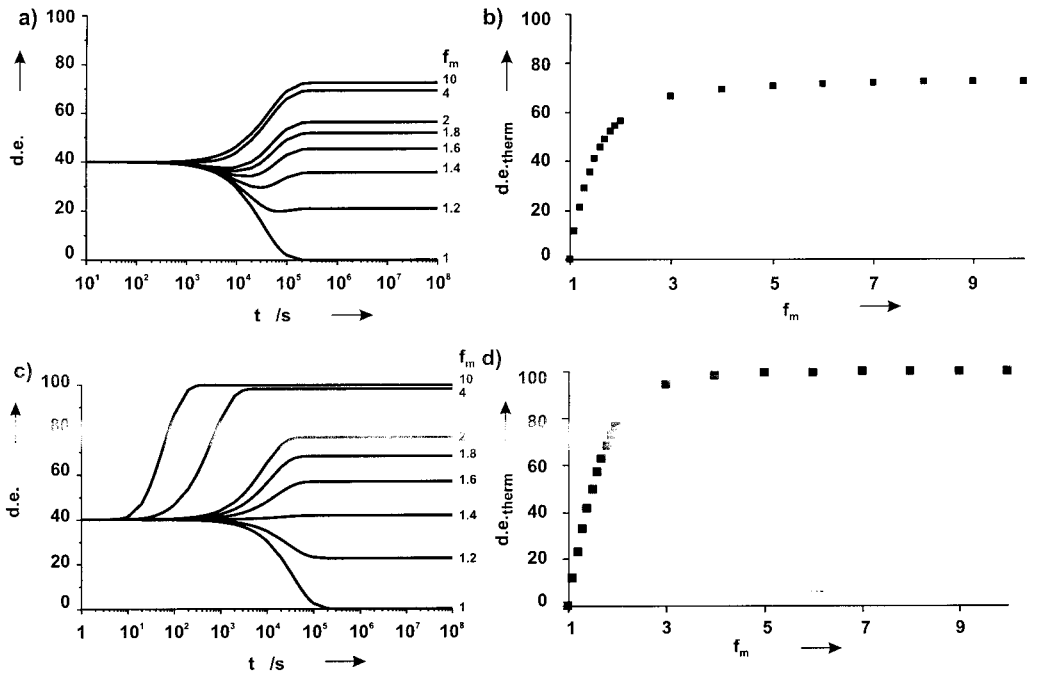

Figure 9. (a) Calculated d.e. as a function of time using model A for different values of f_m (1, 1.2, 1.4, 1.6, 1.8, 2, 4, 10) with $k_{dis,m} = 10^{-5}$ s^{-1} and an initial mole fraction of (*M*)-rosette of 40%. (b) d.e.$_{therm}$ values of (a) versus f_m. (c) Calculated d.e. as a function of time using model B for different values of f_m (1, 1.2, 1.4, 1.6, 1.8, 2, 4, 10) with $k_{dis,m} = 10^{-5}$ s^{-1}, $k_{dis,c} = 0.1$ s^{-1}, and an initial mole fraction of (*P*)-rosette of 40%. (d) d.e.$_{therm}$ values of (c) versus f_m.

dissociation rates are only determined by $k_{dis,m}$, the ratio **1a**:**1b** does not influence t_{init}.

Simulations with model B (Figure 8b) show that the increase in $\Delta\epsilon$ starts much earlier ($t_{init} \approx 10^3-10^4$ s) and that t_{init} is dependent on the amount of *R*CYA present. These observations can be rationalized as follows. In model B the formation of heteromeric assemblies **1c**$_3$•(*R*CYA)$_n$(BuCYA)$_{5-n}$ ($n = 1-5$) occurs via dissociation of *R*CYA and BuCYA components and does not require dissociation of the dimelamines **1c**. Since the dissociation rates for cyanurates ($k_{dis,c} = 10^{-1}$ s^{-1}) are much higher than those for dimelamines ($k_{dis,m}$=10^{-5} s^{-1}), the (*M*)- and (*P*)-diastereomers of the heteromeric assemblies are both populated shortly after mixing. Whereas the (*P*)-diastereomers are stable on this time scale, dimelamine **1c** starts to dissociate

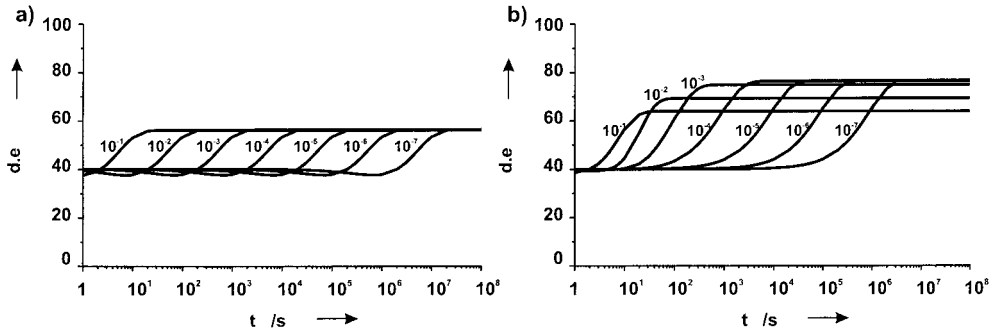

Figure 10. (a) Calculated d.e. in time as a function of k_{dis} using model A for an initial mole fraction of (*M*)-rosette of 40% and $f_m = 2$. (b) Calculated d.e. in time as a function of $k_{dis,m}$ using model B for an initial mole fraction of (*P*)-rosette of 40% and $f_m = 2$ ($k_{dis,c} = 0.1\ s^{-1}$).

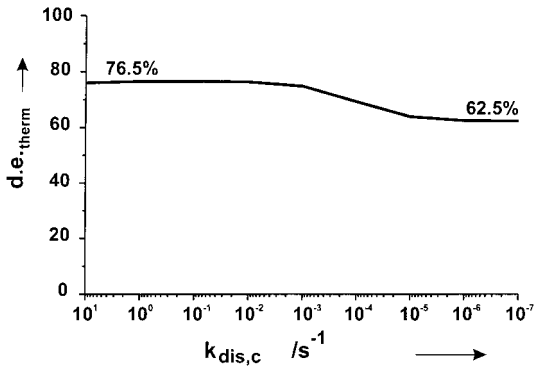

Figure 11. d.e.$_{therm}$ values as a function of $k_{dis,c}$ using model B.

from the less stable (*M*)-diastereomers ($k_{dis,m(M)} > k_{dis,m(P)}$). Consequently, for all ratios chiral:achiral t_{init} is much smaller in model B compared to model A. Furthermore, t_{init} is dependent on the ratio *R*CYA:BuCYA. For high ratios, the concentration of assemblies containing four, five, or six chiral cyanurates is high. The unfavorable (*M*)-diastereomers of these assemblies have a much higher dissociation rate of dimelamines (f_m^4, f_m^5, and f_m^6, respectively), and consequently t_{init} is small. In contrast, for low ratios of *R*CYA to BuCYA the difference in dissociation rates between the (*M*)- and (*P*)-diastereomers is small, and t_{init} is only slightly higher than the corresponding t_{init} obtained in model A. The effect of an increase in f_m on t_{init} in model B can be explained in a similar manner (Figure 9d).

The Value of d.e.$_{therm}$. The most striking differences between the two models are the higher d.e.$_{therm}$ values obtained with model B. Simulations showed that a theoretical limit for the d.e.$_{therm}$ value exists for model A. The reason is that in model A the exchange of chiral and achiral components and (*M*/*P*)-interconversion occur via the same pathway and consequently have the same rate. Therefore, assembly **1b**$_3$·(BuCYA)$_6$ is by definition present as a racemic mixture, which puts a limit to d.e.$_{therm}$ based on the statistical amount of **1b**$_3$·(BuCYA)$_6$ present.

In model B the exchange of chiral and achiral components occurs via a different pathway and with a higher rate than (*M*/*P*)-interconversion. This has a very strong effect on the d.e.$_{therm}$ value. When the exchange of cyanurates is fast compared to the exchange of dimelamines ($k_{dis,c} \gg k_{dis,m}$), all assemblies contain on average the same number of chiral cyanurates. The calculated d.e. for each individual assembly, i.e., **1c**$_3$·(*R*CYA)$_n$(BuCYA)$_{6-n}$ ($n = 0-6$), is *identical for all assemblies*. This includes assembly **1c**$_3$·(BuCYA)$_6$, which does not contain any chiral cyanurates! The *enantiomeric excess* of assembly **1c**$_3$·(BuCYA)$_6$, containing no chiral cyanurates, is equal to the d.e. of assembly **1c**$_3$·(*R*CYA)$_6$ containing six chiral cyanurates (for $f_m = 2$ this is 76%). This can be regarded as another example of chiral memory in a dynamic system.[27,38,39] In theory, this allows a quantitative induction of chirality for all ratios of chiral to achiral, provided that the difference in stability between the (*M*)- and (*P*)-diastereomers containing a single chiral component (parameter f_m) is high enough.

When the difference between $k_{dis,m}$ and $k_{dis,c}$ is smaller, the "memory" effect decreases and the situation shows more resemblance with experiment A. Simulations show that the calculated e.e. for assembly **1c**$_3$·(BuCYA)$_6$ drops significantly (from 76% for $k_{dis,m} = 10^{-5}\ s^{-1}$ to 18% for $k_{dis,m} = 10^{-1}\ s^{-1}$). This is also reflected by the simulations in which $k_{dis,c}$ was lowered (Figure 11). For $k_{dis,c} \leq k_{dis,m}$ exchange of the chiral components is slower than the interconversion of chirality. In that case, the "chiral memory" effect is reduced to 0, which results in values for d.e.$_{therm}$ similar to the values obtained with model A.

Model Assumptions. Both models give a minimal description of the kinetic processes that occur in the mixtures, which is sufficient to simulate and interpret the experimentally obtained data. The assumptions made in the models will be reflected on in this section.

First, it was assumed that dimelamines **1a** and **1b** and cyanurates *R*CYA and BuCYA have equal dissociation rates $k_{dis,m}$ and $k_{dis,c}$, respectively. Unequal rates would result in a nonstatistical distribution between assemblies **1a**$_n$**1b**$_{3-n}$·(BuCYA)$_6$ ($n = 0-3$) and **1c**$_3$·(*R*CYA)$_n$(BuCYA)$_{6-n}$ ($n = 0-6$) favoring the homomeric assemblies. This would result in a lower d.e.$_{therm}$ for both models, since mixing is essential for chiral amplification to occur.

Second, it is assumed that the dissociation rates of cyanurates from the (*M*)- and (*P*)-diastereomers of **1c**$_3$·(*R*CYA)$_n$(BuCYA)$_{6-n}$ ($n = 0-6$) are equal, but in reality these will be different (i.e., $k_{dis,c(M)} > k_{dis,c(P)}$). To account for this difference, a parameter f_c would have to be introduced, which would increase the dissociation rate of *R*CYA depending on the number of *R*CYAs incorporated in the assembly. Incorporation of parameter f_c would only affect the assemblies with unfavorable (*M*)-helicity, i.e., (*M*)-**1c**$_3$·(*R*CYA)$_n$(BuCYA)$_{6-n}$ ($n = 0-6$). However, incorporation of such a parameter f_c in model B in its current form would not be successful for the following reason. The parameter f_c would shift the equilibrium in the model toward the eight-component assemblies (*M*)-**1c**$_3$·(*R*CYA)$_n$(BuCYA)$_{6-n}$ ($n = 1-5$), containing only five cyanurates. Since model B does not allow these assemblies to interconvert directly to the (*P*)-diastereomers, the parameter f_c would cause the concentration of (*M*)-assemblies to be too high. Consequently, a lower d.e.$_{therm}$

(38) Furusho, Y.; Kimura, T.; Mizuno, Y.; Aida, T. *J. Am. Chem. Soc.* **1997**, *119*, 5267−5268.
(39) Yashima, E.; Maeda, K.; Okamoto, Y. *Nature* **1999**, *399*, 449−451.

would be found. This model problem could be circumvented by allowing both the (*M*)- and (*P*)-diastereomers of eight-component assemblies **1c**$_3$·(*R*CYA)$_n$(BuCYA)$_{6-n}$ ($n = 1-5$) to interconvert. In that case, the "true" effect of the parameter f_c would be observed. Within the series (*M*)-**1c**$_3$·(*R*CYA)$_n$-(BuCYA)$_{6-n}$ ($n = 0-6$) the assemblies containing multiple *R*CYAs (e.g., $n = 5, 6$) are more strongly destabilized compared to assemblies containing a few *R*CYAs (e.g., $n = 0, 1$). Effectively, a shift would be observed in the distribution of the (*M*)-diastereomers favoring the assemblies with a few chiral cyanurates. The mass balance requires that this must be accompanied by a similar shift in the distribution of the (*P*)-diastereomers in favor of the assemblies containing multiple *R*CYAs. This would presumably lead to a decrease in the observed d.e.$_{therm}$, since the assemblies (*M*)-**1c**$_3$·(*R*CYA)$_n$-(BuCYA)$_{6-n}$ (e.g., $n = 0, 1$) are only slightly destabilized compared to the corresponding (*P*)-diastereomers.

A third point not included in the model is cooperativity between the chiral centers.[40] Cooperativity would mean that $\Delta G°$ between the (*M*)- and (*P*)-diastereomers increases nonlinearly with the number of chiral centers present. For example, $\Delta G°$ between (*M*)-**1c**$_3$·(*R*CYA)$_6$ and (*P*)-**1c**$_3$·(*R*CYA)$_6$ is larger than $6\Delta G°_{(M/P)}$. In experiment A cooperativity is expected to be negligible, because the chiral centers on the dimelamine components are remote (9.2 Å based on the X-ray crystal structure) and can only indirectly influence each other, taking into account the size of the substituent (~4.5 Å). In experiment B, however, cooperativity may play a role because the chiral cyanurates are pairwise in close proximity (6.4 Å based on the X-ray crystal structure). A nonlinear relation between $\Delta G°$ and the number of chiral centers present, i.e., in the case of cooperativity, would result in smaller t_{init} and higher d.e.$_{therm}$ values in model B. This is caused by the stronger destabilization (higher $k_{dis,m}$) of (*M*)-assemblies containing multiple chiral cyanurates.

Experimental Validation of Models A and B

Fitting of Experiment A. Experiment A was fitted to model A to validate the model and to determine the f_m factor for assemblies **1a**$_n$**1b**$_{3-n}$·(BuCYA)$_6$ ($n = 0-3$). To fit the experimental values, the $\Delta\epsilon$ values have to be interpreted in terms of a d.e. Assuming the same CD activity for the (*M*)- and (*P*)-diastereomers, the data points were independently fitted for each ratio **1a**:**1b** to model A using linear regression by varying $k_{dis,m}$ and f_m, keeping k_{ass} constant (10^5 L·mol^{-1}·s^{-1}). The results of these fits are depicted in Figure 5a (solid lines). Averaging the obtained values for all ratios results in $k_{dis,m} = (4.6 \pm 0.9) \times 10^{-4}$ s^{-1} and $f_m = 5.7 \pm 2.6$. This rate constant is only a factor of 10 higher than the rate constant previously determined for assembly **1c**$_3$·(BuCYA)$_6$ ($k_{obs} = 7.0 \times 10^{-5}$ s^{-1}) by ^{1}H NMR spectroscopy.[27] The value for $f_m = 5.7 \pm 2.6$ corresponds to $-\Delta G°_{M/P}(298\text{ K}) = 4.3 \pm 1.3$ kJ·mol^{-1} for each chiral substituent in the favorable diastereomer. Independently, the $\Delta\epsilon_{therm}$ values (Figure 5c) were fitted to the previously used thermodynamic model which resulted in $-\Delta H°_{M/P}(298\text{ K}) = 2.7 \pm 0.6$ kJ·mol^{-1}. The difference between the two values indicates the different contribution of the entropy term.

Fitting of Experiment B. Experiment B was fitted to model B to validate the model and to determine the f_m factor for assemblies **1c**$_3$·(BuCYA)$_n$(*R*CYA)$_{6-n}$ ($n = 0-6$). As for model A, it was assumed that the (*M*)- and (*P*)-diastereomers have an equal CD activity. In experiment B, chiral amplification occurs so fast that for most ratios *R*CYA:BuCYA intermediate $\Delta\epsilon$ values are not measurable and $\Delta\epsilon_{therm}$ is reached almost instantaneously. Only for a ratio *R*CYA:BuCYA of 10:90 is chiral amplification slow enough to obtain an accurate fit (Figure 5b). Model B requires three parameters, $k_{dis,m}$, $k_{dis,c}$, and f_m, all of which are unknown for this mixture. Therefore, it was assumed that the dissociation rate of dimelamine **1c** is equal to the dissociation rate of dimelamines **1a** and **1b** in experiment A (4.6×10^{-4} s^{-1}). Fitting using linear regression resulted in $k_{dis,c} = 0.26 \pm 0.9$ s^{-1} and $f_m = 2.24 \pm 0.04$.[41] The obtained value for $k_{dis,c}$ is within the range that can be expected for a complex held together by six hydrogen bonds in benzene. The large error in $k_{dis,c}$ is an indication that the kinetic processes incorporated in the model are too limited compared to reality. The value of f_m corresponds to $-\Delta G°_{M/P}(298\text{ K}) = 2.0 \pm 0.05$ kJ·mol^{-1}. The absence of intermediate values for $\Delta\epsilon$ for higher ratios of *R*CYA to BuCYA resulted in unreliable fits. It should be noted though that in general the experimentally observed chiral amplification occurs much faster than predicted by model B. This seems to suggest that cooperativity between chiral centers in fact plays a role in this type of assembly. As discussed previously, cooperativity results in higher d.e.$_{therm}$ values and smaller t_{init} values, because the dissociation rates of dimelamines from the unfavorable (*M*)-diastereomers increases.

Experimental Effect of Changing the Parameter $k_{dis,m}$. Models A and B provide accurate simulations of experiments A and B, respectively. Model B gave surprising novel insights into the Sergeants and Soldiers principle applied to dynamic systems: if the exchange rate of the chiral compounds is faster than the rate of interconversion, a very high d.e.$_{therm}$ can be obtained even when only small amounts of chiral component are present. Additional experiments were performed to support this outcome. The only parameter affecting d.e.$_{therm}$ that can be experimentally altered for an identical mixture, i.e., equal ratio chiral:achiral, is $k_{dis,m}$, since the parameter f_m is entirely determined by the nature of the chemical substituents.

A decrease in temperature results in a decrease in $k_{dis,m}$. Therefore, experiment B was carried out at 70, 60, 50, and 40 °C for four different initial ratios of (*P*)-**1c**$_3$·(*R*CYA)$_6$ and **1c**$_3$·(BuCYA)$_6$. The relative CD intensities at thermodynamic equilibrium (after 1 h) are given in Figure 12a. As predicted by model B, lowering the temperature by 30 °C indeed results in a 4% increase of $\Delta\epsilon_{therm}$. However, the relatively small increase might indicate that $k_{dis,m}$ does not change significantly over this temperature range. An alternative explanation is that at 70 °C $k_{dis,m}$ is already much lower than $k_{dis,c}$. In that case a decrease of $k_{dis,m}$ by lowering the temperature does not have a large effect on $\Delta\epsilon_{therm}$ (see the simulations in Figure 10b).

A second set of Sergeants and Soldiers experiments was performed under conditions in which $k_{dis,m}$ is higher. Previously, we observed that the presence of free barbiturates accelerates the dissociation of dimelamines **1** via the formation of activated complexes. It is assumed that in these complexes partly dissociated melamine fragments are stabilized by the free barbiturates. ^{1}H NMR experiments clearly show that the barbiturates are not incorporated into the assemblies, because of their lower association constants with melamines compared to those of cyanurates (Figure 13). Experiments A and B were carried out in benzene at 70 °C with increasing amounts of DEB present. Plots of the $\Delta\epsilon_{therm}$ values versus the concentration of DEB showed surprising results (Figure 12b). The $\Delta\epsilon_{therm}$ values obtained after mixing (*M*)-**1a**$_3$·(BuCYA)$_6$ and **1b**$_3$·(BuCYA)$_6$

(40) The cooperativity meant here is the synergetic effect of multiple chiral centers in an assembly.

(41) The error corresponds to the standard deviation as calculated by Scientist. A negative value for $k_{dis,c}$ has obviously no physical relevance.

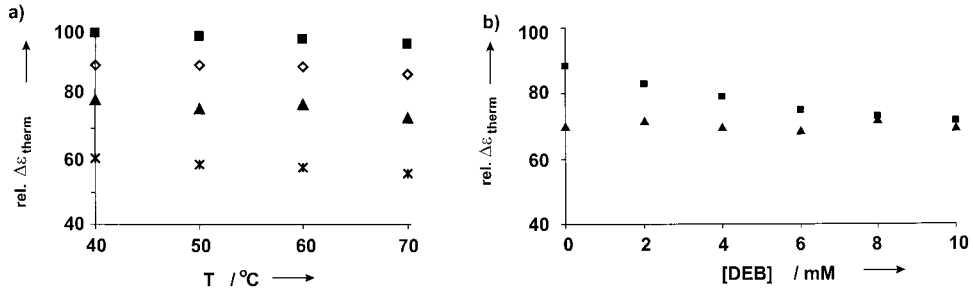

Figure 12. (a) Relative CD intensity at thermodynamic equilibrium as a function of temperature for mixtures of assemblies (*P*)-**1c**$_3$·(*R*CYA)$_6$ and **1c**$_3$·(BuCYA)$_6$ with varying initial mole fractions of (*P*)-**1c**$_3$·(*R*CYA)$_6$ (■, 50%; ◇, 40%; ▲, 30%; *, 20%). (b) Relative CD intensity at thermodynamic equilibrium for mixtures of assemblies (*P*)-**1c**$_3$·(*R*CYA)$_6$ and **1c**$_3$·(BuCYA)$_6$ (■) and (*M*)-**1a**$_3$·(BuCYA)$_6$ and **1b**$_3$·(BuCYA)$_6$ (▲) versus the concentration of DEB. In all cases the mole fraction of chiral component was 40%. All spectra were recorded in benzene at 70 °C.

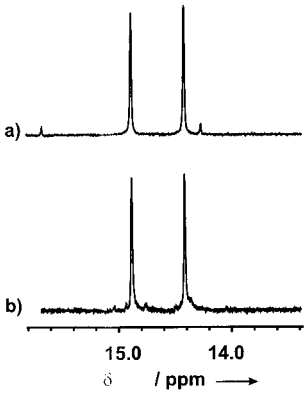

Figure 13. Part of the ^{1}H NMR spectra of assembly **1c**$_3$·(BuCYA)$_6$ (a) without and (b) with 10 mM DEB present. Spectra were recorded in benzene-d_6 at room temperature.

in a 40:60 ratio (experiment A) were identical in the presence and absence of DEB (up to 10 mM). This is in good agreement with model A, which does not predict a dependence of the $\Delta\epsilon_{therm}$ values on $k_{dis,m}$. However, the thermodynamic values obtained after mixing of (*P*)-**1c**$_3$·(*R*CYA)$_6$ and **1c**$_3$·(BuCYA)$_6$ in a 40:60 ratio showed a decrease of 16% in the presence of 10 mM DEB. This is in perfect agreement with model B, which predicted a decrease in d.e.$_{therm}$ upon an increase in $k_{dis,m}$.

Conclusions and Outlook

The experiments and kinetic models presented here gives new insights into the amplification of chirality as applied to dynamic assemblies. If the exchange of chiral components and the interconversion of chirality occur via identical pathways, the d.e.$_{therm}$ value is theoretically limited to a maximum value. The reason is that the assemblies without chiral components are at all times present as a racemic mixture of the (*M*)- and (*P*)-isomers. However, when the exchange of chiral components is much faster than (*M*/*P*)-interconversion, no intrinsic limit exists for the d.e.$_{therm}$ value. The model even predicts that with 1% (or less) chiral component a d.e. higher than 98% can be induced, provided that the f_m value is high enough. Future work will therefore be aimed at the synthesis of chiral cyanurates with a very high f_m value corresponding to a large $\Delta G^\circ_{M/P}$ value. Furthermore, it will be of interest to study the combined chiral amplification and memory effects in other dynamic noncovalent systems.[18,19]

The reported observations also provide interesting perspectives when catalytic reactions in dynamic systems are studied. Using the Sergeants and Soldiers principle, it is possible to bring a large number of achiral components into a chiral microenvironment. When these achiral side chains in the components carry prochiral centers, reactions on these centers could express enantioselectivity.

Experimental Section

The syntheses of compounds **1a**,[25] **1b**,[25] **1c**,[24] **1d**,[24] BuCYA,[25] and *R*CYA[25] have been reported previously. DEB was commercially obtained from Fluka. NMR spectra were recorded on a Varian Unity 300 (^{1}H NMR 300 MHz) spectrometer. CD spectra were recorded on a JASCO J-715 spectropolarimeter.

Assembly Formation. Assemblies were formed by dissolving calix[4]arene dimelamines **1** and the corresponding barbiturates/cyanurates in a 1:2 molar ratio in THF, after which the solvent was evaporated. After being dried under high vacuum, the assemblies were ready for use.

CD Titration Studies. Assembly solutions (1.0 mM) of the homomeric assemblies were mixed in ratios from 90:10 to 10:90 at room temperature and injected into a thermostated cell (0.01 cm) immediately after being mixed. The CD intensities of the mixtures were monitored in time at constant temperatures. The resulting plots were treated as decribed in the text.

Model Simulations. Models A and B were implemented in MicroMath Scientist for Windows, Version 2.01. Text files of the models are provided as Supporting Information.

Acknowledgment. Prof. Feike de Jong is gratefully acknowledged for stimulating discussions. L.J.P. thanks the Council for Chemical Sciences of the Netherlands Organization for Scientific Research (CW-NWO) for financial support.

Supporting Information Available: Models A and B as implemented in MicroMath Scientist for Windows, Version 2.01. This material is available free of charge via the Internet at http://pubs.acs.org.

JA010610E